NON-NEWTONIAN AND THERMAL ELASTOHYDRODYNAMIC ANALYSIS OF THE TRACTION FLUID SANTROTAC 30

A. Campos[1], A. Sottomayor[1], J. Seabra[2]

[1]ISEP, Instituto Politécnico do Porto, R. Dr. António Bernardino de Almeida, 431, 4200-072 Porto, Portugal

[2]Faculdade de Engenharia da Universidade do Porto, R. Dr. Roberto Frias, s/n, 4200-465 Porto, Portugal

ABSTRACT

A thermal and non-Newtonian fluid model under elastohydrodynamic lubrication conditions is proposed, integrating some particularities, such as the separation between hydrodynamic and dissipative phenomena inside the contact. The concept of apparent viscosity is used to introduce the non-Newtonian behaviour of the lubricant and the thermal behaviour of the contact into the Reynolds equation, acting as a link element between the hydrodynamic and dissipative components of the EHD film, independently of the rheological and thermal models considered. The Newton-Raphson technique is used to obtain the lubricant film geometry and the pressure distribution inside the EHD contact. The shear stresses developed in the fluid film are evaluated assuming the non-linear Maxwell rheological model. The surfaces and lubricant temperature distributions are determined using the simplified Houpert's method, applied to the inlet contact zone, and the thermal method proposed by Tevaarwerk is applied in the high pressure contact zone. The model is applied to the analysis of experimental traction curves of a traction fluid measured in a twin-disc machine, obtained for significant ranges of the operating conditions (maximum Hertzian pressure, inlet oil temperature, rolling speed and slide-to-roll ratio). The comparison between model and experimental traction curves showed a very good correlation.

1 INTRODUCTION

The design and development of machine elements are the result of investigations carried through in different scientific areas, in order to satisfy the requirements of the manufacturers in terms of performance, cost and weight. Improvements in lubrication heat reduction and load capacity enhancement are some of the areas with interest to this work.

The presence of a lubricant between two rolling / sliding bodies introduces a fluid body that transmits the load between these two elements ensuring that the contact does not occur. This concern in a so called elastohydrodynamic lubricated contact. The generated film thickness of an elastohydrodynamic contact depends mainly on the surface velocity, lubricant properties and lubricant rheological behavior at the temperatures occurring inside the contact. The lubricant film stops the metal on metal contact whilst reduce friction between surfaces in relative movement.

The proposed thermal and non-Newtonian fluid model under elastohydrodynamic lubrication using de concept of the apparent viscosity enables the application of the rheological model better adapted to each lubricant, without appealing to numerical model modifications. This numerical model can be used to estimate film thickness and friction forces, allowing to predict optimum operating conditions in mechanisms involving the EHD lubrication. A traction

drive is a power transmission mechanism which operates smooth and quietly, involves EHD lubrication. The Santotrac 30 is a traction fluid applied in this kind of mechanisms. His traction behaviour is simulated by the developed numerical model and compared with experimental data obtained in a twin disc machine. The conditions found inside the contact, such as film thickness, temperatures and pressures are also analyzed depending on operating conditions.

2 ELASTOHYDRODYNAMIC LUBRICATION: GOVERNING EQUATIONS

In solving a thermal and a non-Newtonian elastohydrodynamic problem, the coupled Reynolds equation, the film geometry equation, the load balance equation, the energy equation and the lubricant rheological model must be considered.

2.1 Reynolds equation

Assuming a Newtonian behaviour of the lubricant and taking into account the normal simplifications to the Navier-Stokes equations applied to the elastohydrodynamic lubrication problem, the Reynolds equation for an infinitely long contact (on Oy direction) can be expressed as ([1] and [2]):

$$\frac{\partial}{\partial x}\left(\frac{\partial p}{\partial x}\frac{\rho}{12\eta}h^3\right)=\frac{(U_1+U_2)}{2}\frac{\partial}{\partial x}(\rho h) \qquad (1)$$

2.2 Film geometry equation

The lubricant in the contact neighbourhood is drawn inside being squeezed and stretched. The generated hydrodynamic pressure is high enough to cause appreciable elastic deformation of the solids surfaces and also causes lubricant viscosity and density changes. In defining the lubricant film geometry it is necessary to include the elastic deformation in the free load surfaces geometry. Attempting to figure 1, the film geometry can be defined by the expression:

$$h(x)=h_c+[\bar{u}_z(x)-\bar{u}_c]+h^0(x) \qquad (2)$$

where $\bar{u}_z$ is the normal displacement of any surface point being submitted to the pressure p(x) and obtained by ([3] and [4]):

$$\bar{u}_{zi}(x)=-\frac{2\left(1-\upsilon_i^2\right)}{\pi E_i}\int_{-b1}^{b2} p(s)\ln|x-s|ds+C \qquad (3)$$

The lubricant film geometry, defined in equation (2), can be rewritten as:

$$h(x)=h_c+h^0(x)-\frac{2}{\pi E'}\int_{-b_1}^{b_2} p(s)\ln(x-s)^2\,ds \qquad (4)$$

2.3 Force balance equation

The normal force applied to the contact is supported by the hydrodynamic pressure generated in the contact. So, the equilibrium equation can be written:

$$F_z=\int p(x)\,dx$$

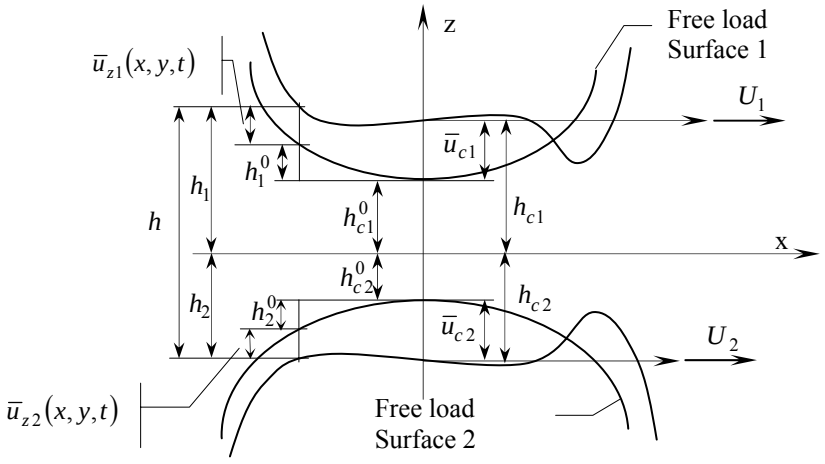

Fig 1 – Film geometry definition.

2.4 Force balance equation

The normal force applied to the contact is supported by the hydrodynamic pressure generated in the contact. So, the equilibrium equation can be written:

$$F_z = \int p(x)\,dx \tag{5}$$

2.5 Energy balance

Predicting the temperature rise inside the contact is one of the most important aspects in elastohydrodynamic lubrication. Locally, this knowledge allows to evaluate the lubricant properties and to state the lubricant rheological behaviour. Consequently, the film geometry and the pressure distribution will be also affected. Globally, it is possible to estimate the dissipated energy by the contact.

Figure 2 presents the scheme applied to the thermal contact analysis, allowing the surfaces and lubricant temperatures evaluation and also the heat flows to each surface.

2.5.1 Energy equation applied to the lubricant

The temperature profile for the lubricant film can be solved by the energy equation associated with appropriate boundary conditions and assuming some simplifying hypothesis. The energy equation for line contact problems may be written as ([5] and [6]):

$$\frac{\partial^2 T_F}{\partial z^2} + \frac{\phi(x,y,z)}{k_F} = \left(\frac{\rho c_{pF}}{k_F}\right) U_M \frac{\partial T_F}{\partial x} \tag{6}$$

2.5.2 Energy equation applied to the solids

It is possible to reduce the thermal problem of two solids in contact and in relative movement, to the problem of a heat source in movement in an infinite half-space. The contact plan is considered adiabatic, with exception to the heat source area [6], admitting that: (i) the solids become deformed in a purely elastic way and are isotropic, (ii) the viscous heating is not significant, (iii) the compression heating is also not significant and (iv) the speed in the rolling direction only exists on Ox direction (= > v=w=0). Therefore, under these conditions, the energy equation for the solids can be written as [6],

$$\frac{\partial^2 T_i}{\partial x^2} + \frac{\partial^2 T_i}{\partial y^2} + \frac{\partial^2 T_i}{\partial z^2} = \alpha_{si} U_i \frac{\partial T_i}{\partial x} \tag{7}$$

2.5.3 Energy balance in the contact inlet

In the inlet contact zone or low pressure zone, a lubricant back-flow region is generated ([7] and [8]), due to the fast variation of geometry, the increasing pressure and the surfaces speeds, modifying the speed profile in each section. Thus, the evaluation of the temperature rise in the inlet zone is obtained from the simplified Houpert's method [7], but considering the temperature rise of each surface. The expression for the temperature rise in each point is:

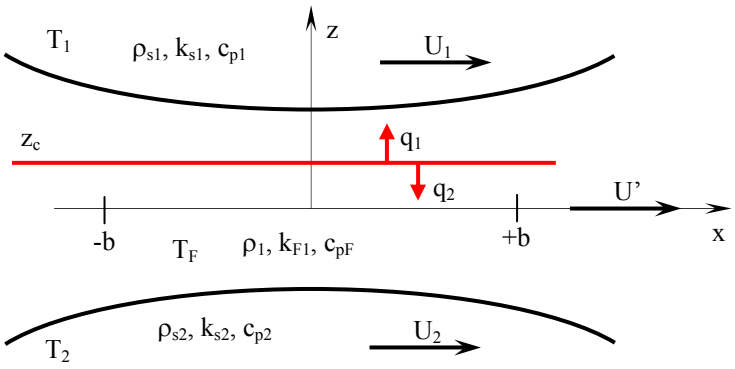

Fig 2 – The thermal problem analysis.

$$\Delta T_{cc} = \frac{\Delta T_{sc} + \frac{\rho.c_{pF}}{k_F}\frac{\Delta T_1.h^2}{(x_2 - x_1)} \times C}{1 + \frac{\rho.c_{pF}}{k_F}\frac{h^2}{(x_2 - x_1)} \times C} \quad (8)$$

where

$$\Delta T_{sc} = \frac{1}{192}\frac{h^4}{k_F\,\eta}\left(\frac{dp}{dx}\right)^2 + \frac{h^3}{24k_F}\frac{dp}{dx}\left(\frac{U_2 - U_1}{h}\right) + \frac{1}{8}\frac{h^2\eta}{k_F}\left(\frac{U_2 - U_1}{h}\right)^2 \quad (9)$$

and

$$C = -\frac{9}{960\,\eta}h^2\frac{dp}{dx} + \frac{5U_1}{96} + \frac{U_2}{32} \quad (10)$$

2.6 Lubricant rheology

2.6.1 Apparent viscosity

The Reynolds equation was deduced admitting a Newtonian behaviour for the lubricant. In order to introduce the non-Newtonian and thermal effect in the Reynolds equation, the viscosity in each point is acquired from the assigned apparent viscosity, and not using a state viscosity equation. The apparent viscosity is defined by the equation

$$(\eta_{ap})_i = \frac{\tau_i}{\dot{\gamma}_i} = \frac{\tau_i}{(U_1 - U_2)/h_i} \quad (11)$$

which incorporates the non-Newtonian shear stresses applied to the lubricant, at the lubricant temperature, in each point inside the contact.

2.6.2 Shear stresses

The shear stresses are calculated considering the rheological model better adjusted to each lubricant, taking into account the operating conditions. The shear stresses are obtained considering the Maxwell's model, which admits the total shear strain rate is the sum of two components: a viscoelastic term and a viscous term. This relation can be written as:

$$\dot{\gamma} = \dot{\gamma}_e + \dot{\gamma}_v \quad (12)$$

From experimental results Bair and Winer ([1] [2]) concluded that viscous term can be described by a simple natural logarithm function. This result in a new relation based on the Maxwell's:

$$\dot{\gamma} = \frac{\dot{\tau}}{G_F(p,T)} - \frac{\tau_L}{\eta(p,T)}\ln\left(\frac{\tau}{\tau_L}\right) \quad (13)$$

where τ_L is the limit shear stress, which is function of the pressure and the temperature, such as G_F and η.

3 NUMERICAL MODEL

The developed numerical model allows the analysis of Hertzian line contacts lubricated or EHD line contact, incorporating the variation of temperature and the non-Newtonian behaviour of the lubricant.

In the attainment of the pressure profile and the film geometry the method of Newton-Raphson is applied, considering a Newtonian Reynolds equation [10].

The numerical model, making use of the apparent viscosity, express in a simple and expedite way to introduce the non-Newtonian effects in the Reynolds equation, without being necessary to appeal to the modified forms of this equation for the inclusion of the rheological models.

The numerical solution of the energy equation applied to the lubricant is obtained through the Laplace transform as delineated by Carslaw and Jaeger [9] and presented by Tevaarwerk [5]. Carlslaw and Jaeger also supply the solution for the surfaces temperature definition.

The implemented algorithm has an initialization block and two main blocks, as shown in figures 3 and 4. The algorithm starts defining the problem in analysis introducing the lubricant and the bodies in contact characteristics. These input data is applied to produce the initial conditions (see figure 3).

The two main blocks: block 1 for the lubricant film geometry and the pressure profile calculation (figure 4-block 1); and block 2 for the lubricant shear stress and the temperature profiles evaluations (figure 4-block 2).

Defined the initial conditions the algorithm enters first in block 2 (figure 4- block 2), where is gotten the shear stress, allowing the calculation of the wasted power, the internal waste, the heat flow to the surfaces. It is then possible to evaluate the temperature profiles for the surfaces and subsequently the lubricant temperature profile. After convergence in the block 2 the algorithm passes to the block 1 for the film geometry and pressure profile evaluations (figure 4- block 1), imposing the lubricant temperature and shear stress profiles. This allows the viscosity calculation to be made by the definition of the apparent viscosity, as defined for the equation (4). After the simultaneous convergence in the two blocks a solution is obtained for the proposed contact analysis.

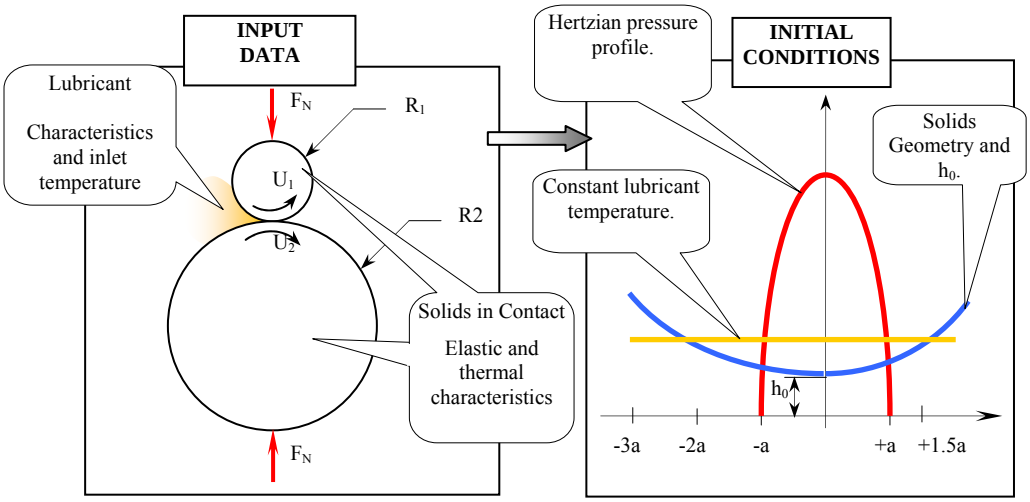

Fig 3 – Numerical model: input data and initial conditions.

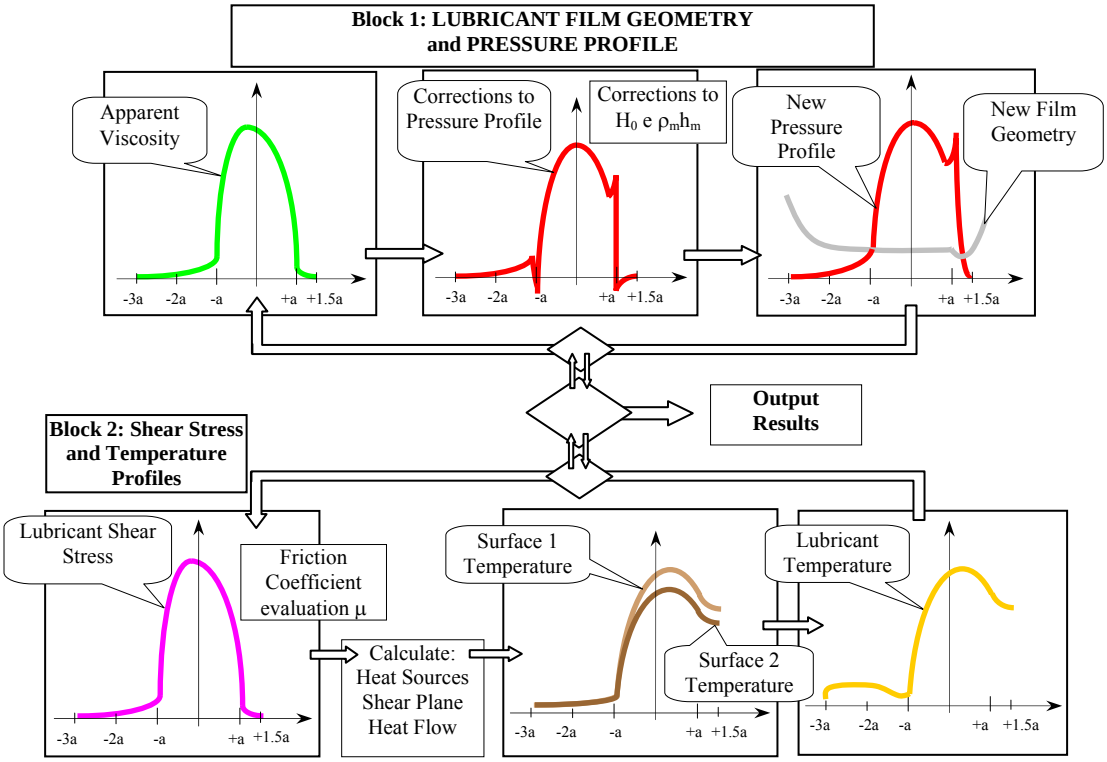

Fig 4 – Numerical model: block 1, lubricant film geometry and pressure profile and block 2, lubricant shear stress and temperature profiles.

4 TRACTION CURVES, CONTACT TEMPERATURES AND FILM THICKNESS RESULTS FOR SANTROTAC 30 FLUID

The numerical model was used to determine the traction curves of the Santotrac 30 traction fluid. The numerical results are compared with the experimental values, registered in a twin disc machine by Gupta et al. [11].

Figure 5 shows the working principle of the twin-disc machine: two discs, with the macro and micro geometries perfectly known, with independent speeds, are placed in contact imposing a normal force, simulating the desired operating conditions. This contact is lubricated with the fluid at constant temperature.

The elastic and thermal characteristics of the discs and their geometry are presented in Table 1.

4.1 Lubricant properties and rheological parameters

Gupta et al. [11] assumed the following lubricant properties:

Kinematic viscosity (cSt),

$$\log_{10}\log_{10}(\upsilon+0.80) = -4.10\log_{10}T + 10.31 \quad (14)$$

Piezoviscosity coefficient (Pa^{-1}),

$$\alpha_\eta = 2.90\times10^{-8}\exp\left[-8.318\times10^{-3}\times(T-277.8)\right] \quad (15)$$

Density-temperature relation ($x10^3$ kg/m^3),

$$\rho = 0.817 + 6.66\times10^{-4}(422.22 - T) \quad (16)$$

Thermal conductivity (N/s/ºC)

$$k_F = 0.109 - 1.71\times10^{-5}(T-311.1)^{1.322} \quad (17)$$

and a specific heat equal 2000 J/(kg.ºK).

Sottomayor [12], admitting a viscoelastic-plastic behaviour for this fluid and exponential laws for the variation of the shear modulus (G_L) and of the limiting shear stress (τ_L) with pressure and temperature, proposed the values shown in table 2 for the rheological parameters.

4.2 Contact operating conditions

Table 3 shows the operating conditions applied to the twin-disc contact: inlet lubricant temperatures, maximum Hertzian pressures and kinematics.

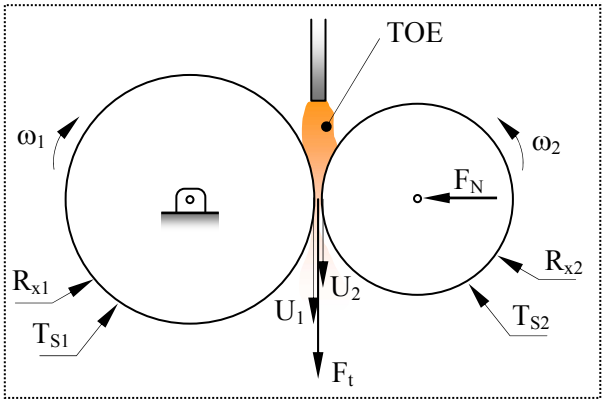

Fig 5 – Working principle of a twin disc machine.

Table 1 – Discs geometry and elastic and thermal characteristics [11].

Parameter	Value	Units
$E_1 = E_2$	$210x10^{-9}$	[Pa]
$\nu_1 = \nu_2$	0.3	[---]
$c_{pS1} = c_{pS2}$	460	[J/(kg.ºK)]
$k_{s1} = k_{s2}$	46	[W/(m.ºK)]
$\rho_{S1} = \rho_{S2}$	7800	[kg/m^3]
R_{x1}	50.8	[mm]
R_{x2}	50.8	[mm]

4.3 Contact operating conditions

Table 3 shows the operating conditions applied to the twin-disc contact: inlet lubricant temperatures, maximum Hertzian pressures and kinematics.

4.4 Numerical vs. experimental traction curves

Figure 6 compares the tractions curves obtained by the numerical model (lines) with the experimental traction values (points) [11], showing that the model describes quite well the influence of the operating conditions on the fluid traction curves. The main effects are:

- The friction coefficient increases when the applied load increases.
- The friction coefficient decreases when the entraining speed (U_M or U_T) increases.
- For very low slide-to-roll ratios VE, the friction coefficient increases when VE increases.
- For higher values of slide-to-roll ratios, the power dissipation inside the contact becomes very significant and, consequently, the friction coefficient

remains constant or even decreases when VE increases, depending on the applied load and operating speed.

A 97.80% correlation was obtained between the numerical and experimental friction coefficient values.

Table 2 – Shear modulus (G_L) and limiting shear stress (τ_L) for Santotrac 30 fluid considering a viscoelastic-plastic behaviour [12].

$G_F = G_0 \times \exp\left[\alpha_G \times p + \beta_G \times \left(\frac{1}{T} - \frac{1}{T_0}\right)\right]$			$\tau_L = \tau_{L0} \times \exp\left[\alpha_{\tau L} \times p + \beta_{\tau L} \times \left(\frac{1}{T} - \frac{1}{T_0}\right)\right]$			
G_0 [Pa]	α_G [Pa^{-1}]	β_G [ºK]	τ_{L0} [Pa]	α_{τ_L} [Pa^{-1}]	β_{τ_L} [ºK]	T_0 [ºK]
$0.24410 \times 10^{+06}$	6.3691×10^{-09}	$7.0000 \times 10^{+03}$	$53.185 \times 10^{+06}$	0.0	$0.76875 \times 10^{+03}$	323

Table 3 – Contact operating conditions for Santotrac 30 fluid [11].

Inlet oil temperature (TOE) [ºC – ºK]	Maximum hertzian pressure (P0) [GPa]	Sliding rate (VE) [%]	Means speed (U_M) [m/s]
70.5 – 344	0.570	≈ 0	21.17
105 – 378	0.913	a ≈ 10	45.53

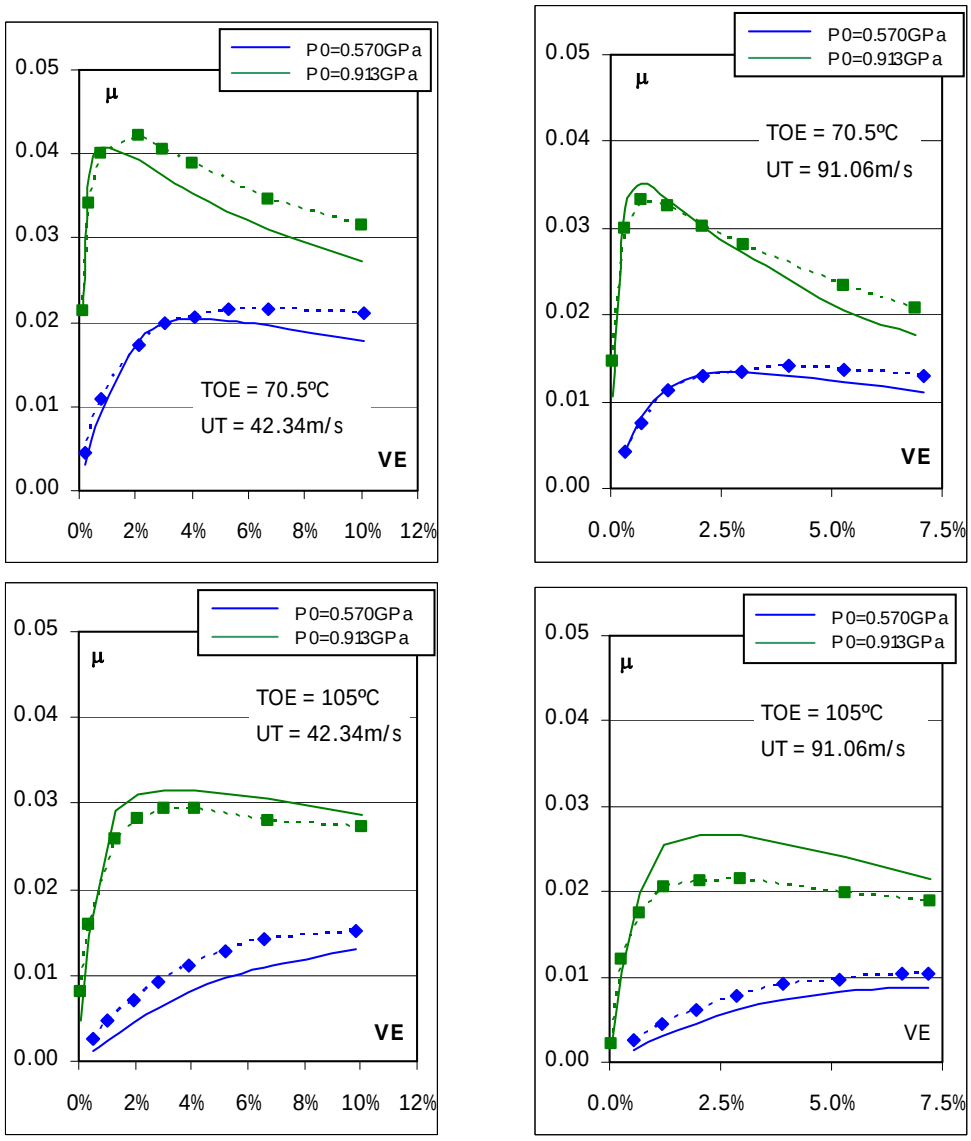

Fig 6 – Experimental vs. numerical tractions curves for Santotrac 30 fluid.

4.5 Lubricant temperatures

Figure 7 presents the maximum temperature rise achieved by the lubricant in the contact inlet (ATF_{max}-Conv) and inside the high pressure zone or Hertzian zone (ATF_{max}-ZAP), for different operating conditions. Several considerations might be pointed out from Figure 7:

- The lubricant temperature rise in the contact inlet (ATF_{max}-Conv) is almost independent of the applied load (or maximum Hertzian pressure), but strongly dependent on the entraining speed and it decreases when the lubricant inlet temperature (TOE) increases. When the slide-to-roll ratio increases the lubricant temperature rise in the contact inlet (ATF_{max}-Conv) is small (a few degrees Celsius).
- In the high pressure zone the lubricant temperature rise (ATF_{max}-ZAP) is strongly dependent on the applied load, since this zone supports almost the total load, but almost independent of the entraining speed. The lubricant film is submitted to high contact pressures and significant slide-to-roll ratios in this zone, generating an important power dissipation that heats the lubricant.

In both zones, the maximum temperature rise decreases when the inlet oil temperature (TOE) increases. In fact, for higher inlet oil temperatures the power dissipation inside the contact is smaller, the heat evacuated to the metallic surfaces decreases and the lubricant temperature rise is smaller.

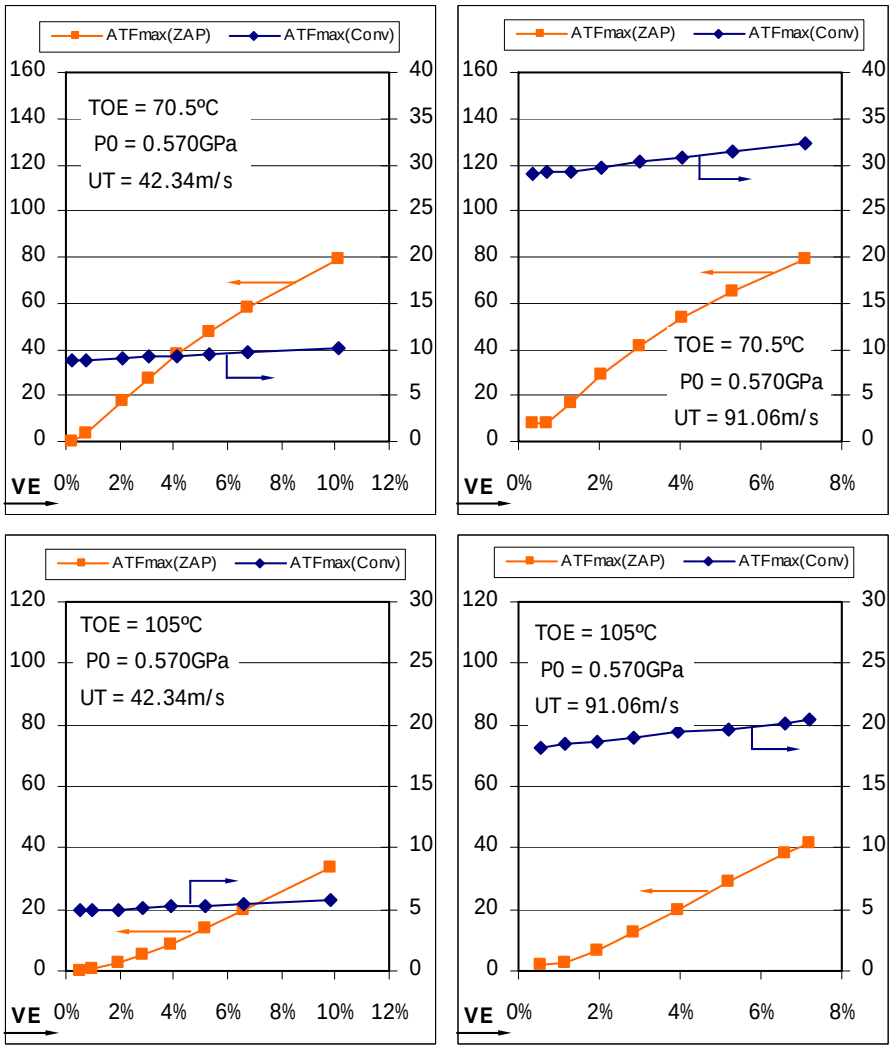

Fig 7 – Lubricant maximum temperature rises in the convergent (ATFmax-Conv) and in the high pressure zone (ATFmax-ZAP).

4.6 Lubricant film geometry

Figure 8 presents the influences of the operating conditions on the lubricant film geometry. The most important effects are:

- When the entraining speed increases a global increase of the film thickness is determined, as expected (see Figure 8 [a] and [b]). The centre film thickness rises and the minimum film thickness, at the contact outlet, looses its importance. The increase in centre film thickness might be more or less significant depending on the temperature rise inside the contact inlet (see Figure 7).
- The influence of the slide-to-roll ratio on the lubricant film geometry, happens in two main locations depending on the operating conditions. In the transition zone from the convergent to the high pressure zone (see Figure 8 [a] and [b]) the temperature rise in the convergent affects the pressure generation in that transition zone and the centre film thickness decreases when the slide-to-roll ratio increases. In the high pressure zone, higher slide-to-roll ratios generate higher lubricant temperatures, consequently the lubricant density decreases and the film thickness rises in order to maintain the product ρh constant (see equation 1), that is maintain the hydrodynamic flow (see Figure 8 [c] and [d]).
- When the inlet oil temperature (TOE) increases the lubricant viscosity drops, the hydrodynamic pressure generation in the convergent decreases and, consequently, a global reduction of the thickness takes place (see Figure 8 [c] and [d]).

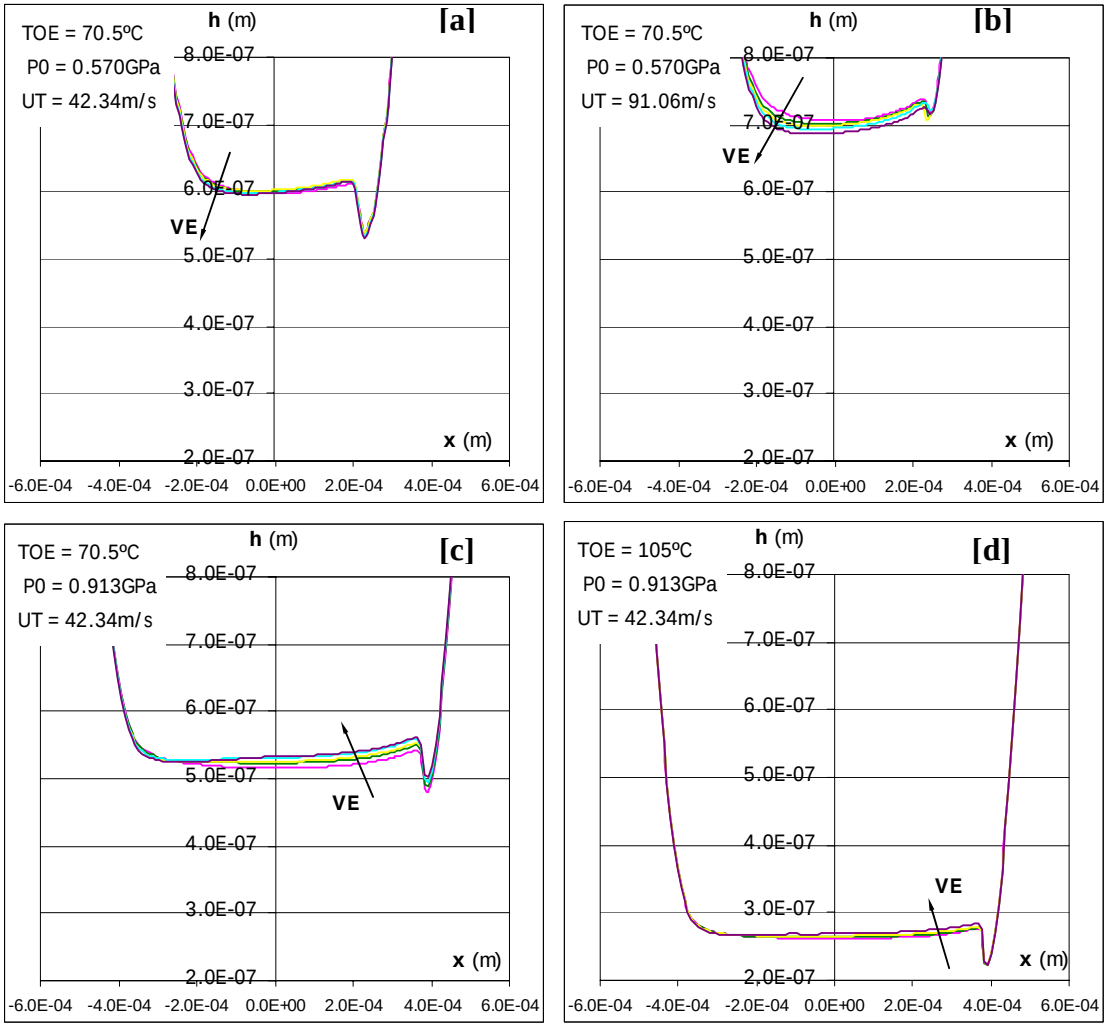

Fig 8 – Lubricant film geometry for several operating conditions (arrows indicate the slide-to-roll ratio raise).

The influence of the operating conditions and of the lubricant temperature variations on the lubricant film geometry can be represented by the shear thinning factor, ϕ_T, which is the ratio between the central film thickness in real conditions and the central film thickness considering the contact isothermal:

$$\phi_T = \frac{h_{0T}}{h_{0\,Isot}} \tag{18}$$

Figure 9 shows the shear thinning factor ϕ_T for all the operating conditions considered:

- When the entraining speed raises the shear thinning parameter decreases very significantly, mainly when the inlet oil temperature is low, implying a significant reduction of the centre film thickness when compared to the corresponding isothermal value, due to the lubricant temperature rise in the contact convergent.
- The shear thinning factor (ϕ_T) increases when the inlet oil temperature (TOE) increases, but this effect only becomes important for high entraining speeds.
- The influence of the load, or Hertzian pressure, on the shear thinning factor (ϕ_T) is almost unnoticed, unless for very low values of the slide-to-roll ratios (VE).

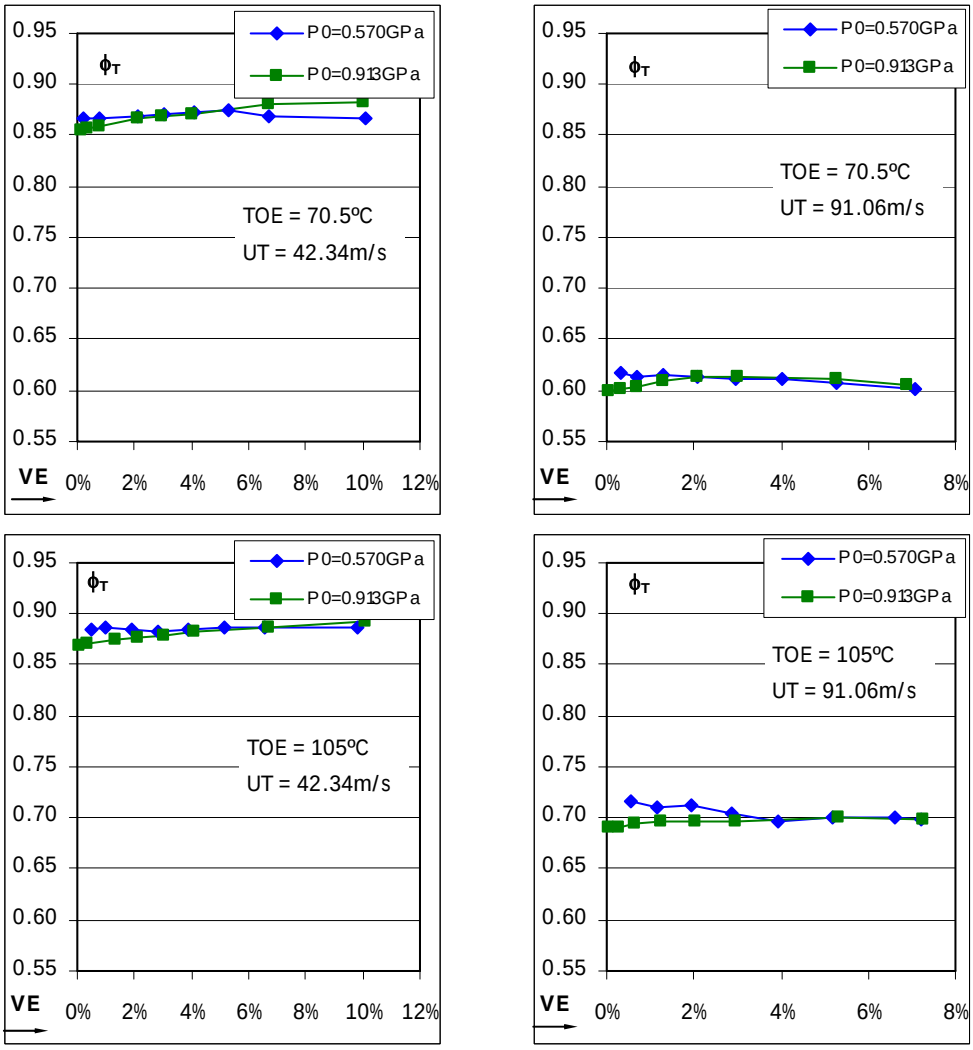

Fig 9 – Shear thinning factor ϕ_T.

4.7 Pressure and shear stresses profiles

Figure 10 shows the normal pressure and shear stress profiles, considering an inlet oil temperature of 70.5ºC and an entraining speed of 42.43m/s, for two different values of the maximum Hertzian pressure, 0.570 GPa and 0.913 GPa, and increasing slide-to-roll ratios.

The pressure profiles are not affected by the speed, by the slide-to-roll ratio or by the inlet oil temperature. The maximum Hertzian pressure and the contact width increase, as expected, when the applied load increases (see Figure 10 [a] and [b]).

The shear stress profiles are very significantly affected by the slide-to-roll ratio (VE). For the lower Hertzian pressure value (0.570GPa - Figure 10 [a]) the maximum shear stress increases when VE increases.

For higher Hertzian pressure value (0.913GPa - Figure 10 [b]), the power dissipation inside the contact becomes more important. Consequently, the lubricant temperature increases very significantly, affecting the lubricant properties, and the maximum shear stress in the lubricant film decreases while VE is increasing.

For the higher value of the Hertzian pressure 0.913 GPa (see Figure11) the shear stress profile is controlled by the limiting shear stress (τ_L) of the lubricant, which decreases as the slide-to-roll ratio increases, due to increasingly higher lubricant temperatures.

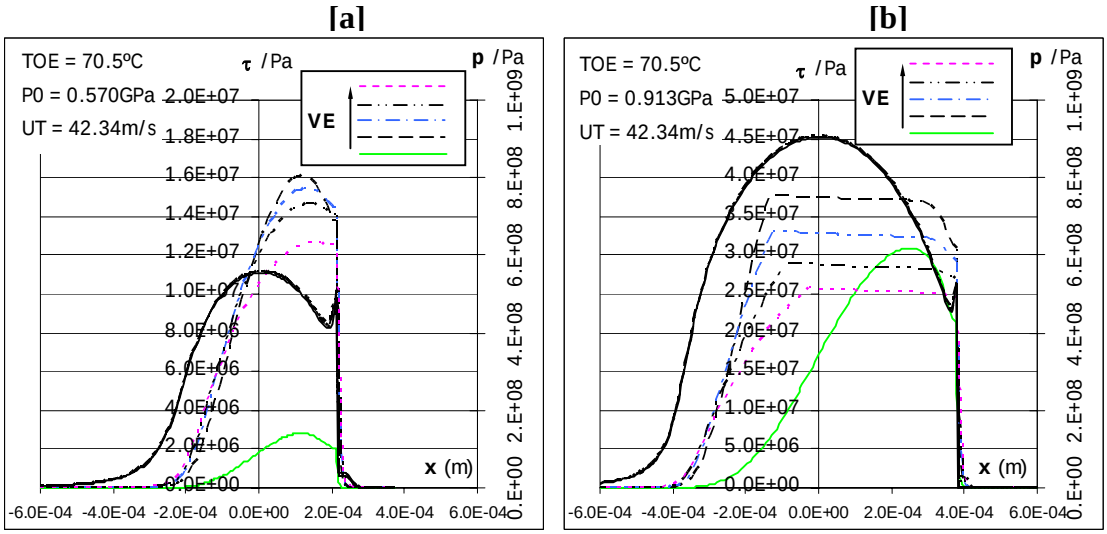

Fig 10 – Pressure and shear stresses profiles for TOE = 70.5ºC, UT = 42.3m/s considering P0 = 0.570 GPa and 0.913 GPa.

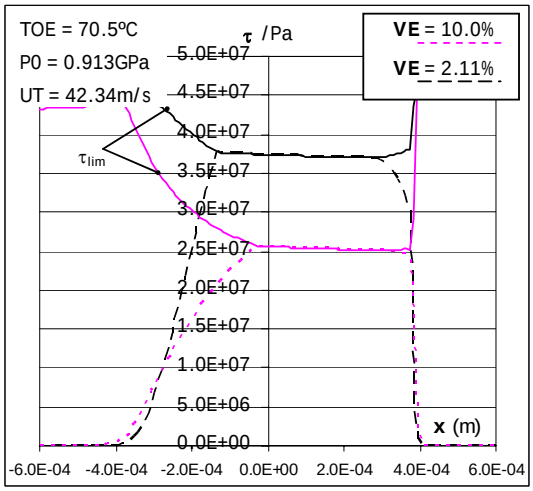

Fig 11 – Lubricant shear stress limit for TOE = 70.5ºC, UT = 42.3m/s and P_0 = 0.913 GPa.

5 CONCLUSIONS

The numerical model used to determine the traction curves of the Santotrac 30 proved to be very efficient, generating values very similar to those measured experimentally by Gupta et al. [11] in a twin-disc machine.

The non-Newtonian and thermal EHD analysis of the twin-disc contact lubricated with the Santotrac 30 fluid shows the following characteristics:

1. Inlet oil temperature (TOE = 70.5 ºC and 105 ºC):
   - The influence of the slide-to-roll ratio is smaller for higher inlet oil temperatures.
   - When the inlet oil temperature increases the lubricant film thickness decreases.
   - The inlet shear thinning effect is smaller for higher inlet oil temperatures.
2. Maximum Hertzian pressure (P_0 = 0.570 GPa and 0.913 GPa):
   - Higher maximum contact pressures generate higher lubricant temperatures in the Hertzian contact zone.
   - The maximum contact pressure doesn't affect the temperature raise in the convergent.
   - Within the ranges of operating conditions considered, the maximum Hertzian pressure has a small influence on the shear thinning factor, ϕ_T.
3. Slide-to-roll ratio (VE $\approx$ 0 to $\approx$ 10%):
   - The slide-to-roll ratio has a modest influence on the lubricant temperature increase in the contact inlet. On the opposite, the influence of VE on the lubricant temperature in the high pressure zone is very important.
   - High slide-to-roll ratios, generate a very strong power dissipation inside the contact and a high increase of the lubricant temperature, leading to the degradation of the lubricant properties and a significant reduction of the shear stresses inside the contact.
4. Entraining speed (UT = UM x 2 = 42.34m/s and 91.06m/s):
   - The increase of the entraining speed imposes a significant increase of the lubricant temperature, both in the convergent and in the high pressure zone. This also contributes to the degradation of the lubricant properties and the decrease of the shear stresses that the lubricant can accommodate.
   - When the entraining speed grows a global increase of the lubricant film thickness occurs and the minimum lubricant film thickness looses its importance.
   - The shear thinning factor, ϕ_T, decreases very significantly when the entraining speed increases.

REFERENCES

[1] R. Gohar, "Elastohydrodynamics", Ellis Horwood Limited, Chichester, 1988.

[2] K B.J. Hamrock, "Fundamentals of Fluid Film Lubrication", McGRAW-HILL International Editions, 1994.

[3] K.L. Johnson, "Contact Mechanics", Cambridge University Press, 1985.

[4] S.P. Timoshenko e J.N. Goodier, "Theory of elasticity", Mc Graw-Hill, International Student Edition, 1970.

[5] J.L. Tevaarwerk, "Traction calculations using the shear plane hypothesis", Proc. Of Leeds-Lyon Symposium on Tribology, Paper VIII(iii), pp. 201-215, 1979.

[6] L. Bordenet, J.P. Chaomleffel e G. Dalmaz, "Le contact elastohydrodynamique ponctuel lubrifié par un fluide newtonien: modele thermique simplifie", Publicação do Laboratoire de Mécanique des Contacts – INSA de Lyon, 37 p., França, 1991.

[7] L. Houpert, "Contribution a l'etude du frottement dans un contact elastohydrodynamique", Tese de Doutoramento, IDI 3-8019, INSA, Lyon, 1980.

[8] S. Wang, C. Cusano e T. F. Conry, "Thermal Analysis of Elastohydrodynamic Lubrication of Line Contacts Using the Ree-Eyring Fluid Model", ASME Journal of Tribology, Vol. 113, p. 232, 1991.

[9] H.S. Carslaw e J.C. Jeager, "Conduction of heat in solids", Oxford Science Publications, 2ª Edição, Oxford, UK, 1959.

[10] L.G. Houpert e B.J. Hamrock, "Fast Approach for Calculating Film Thickness and Pressures in Elastohydrodynamically Lubricated Contacts at High Loads", ASME Journal of Tribology, Vol. 108, p. 411, 1986.

[11] P.K. Gupta, L. Flamand, D. Berthe e M. Godet, "On the tractions behavior of several lubricants", Transactions of the ASME, Journal of Lubrication Technology, 80 – C2/Lub - 15, 1980.

[12] A. Sottomayor, "Reologia de um lubrificante não-Newtoniano no interior de um contacto termoelasto-hidrodinâmico. Determinação dos parâ-metros reológicos de um lubrificante", Tese de Doutoramento, DEMEGI, Faculdade de Engenharia da Universi-dade do Porto, Porto, Portugal, 2002.

NOMENCLATURE

a	=	Hertzian Contact semiwith (Ox)	m
ATF	=	Lubricant temperature increase	ºK ou ºC
c_{pF}	=	Specific heat of the lubricant	J/(kg.ºK)
c_{pS}	=	Specific heat of the solids	J/(kg.ºK)
$E_{1,2}$	=	Modulus of elasticity 1,2	Pa
F_z	=	Normal force applied to the contact	N
G_F	=	Shera modulus of elasticity	Pa
h	=	Lubricant film thickness	m
h_c	=	h_0, Film thickness at the conatct centre	m
h^0	=	Undeformed geometry of the solids	m
k_F	=	Lubricant thermal conductivity	W/(m.ºK)
k_S	=	Solids thermal conductivity	W/(m.ºK)
p	=	Pressure	Pa
P_0	=	Maximum contact pressure	Pa
T	=	Temperature	ºK ou ºC
TOE	=	Inlet lubricant temperature	ºK ou ºC
ΔT_{sc}	=	Temperature increase without convection	ºK ou ºC
ΔT_{cc}	=	Temperature increase with convection	ºK ou ºC
$U_{1,2}$	=	Surface velocity	m/s
U_M	=	$(U_1+U_2)/2$ = Rolling speed	m/s
U_T	=	(U_1+U_2) = Total speed	m/s
VE	=	$(U_1-U_2)/(U_1+U_2)$ = Slide to roll ratio	----
x	=	Rolling direction	m
z	=	Film thickness direction	
$\dot{\gamma}$	=	Shear rate	s^{-1}
η	=	Dynamic viscosity	Pa.s
ρ	=	ρ_F = Specific mass of the Lubricant	kg/m^3
τ	=	Shear stress	Pa
τ_L	=	Limiting shear stress of the lubricant	Pa